Microelectronics Reliability xxx (2017) xxx–xxx

Contents lists available at ScienceDirect

Microelectronics Reliability

journal homepage: www.elsevier.com/locate/microrel

Practical quantitative scanning microwave impedance microscopy

Oskar Amster [a,*], Fred Stanke [a], Stuart Friedman [a], Yongliang Yang [a], St.J. Dixon-Warren [b], B. Drevniok [b]

[a] PrimeNano, Inc., 8701 Patrick Henry Dr., Bldg 8, Santa Clara, CA 95054, USA
[b] TechInsights, 1891 Robertson Road, Ottawa, Ontario K2H 5B7, Canada

ARTICLE INFO

Article history:
Received 27 May 2017
Received in revised form 17 July 2017
Accepted 18 July 2017
Available online xxxx

Keywords:
Scanning microwave impedance microscopy
Scanning microwave microscopy
Nanoscale C-V curves
Electrical characterization doping concentration

ABSTRACT

Scanning microwave impedance microscopy (sMIM) is an emerging technique that has the potential to displace conventional scanning capacitance microscopy (SCM), and other electrical scanning probe microscopy (SPM) techniques, for the profiling of dopants in semiconductor samples with sub-micron spatial resolution. In this work, we consider the practical application of sMIM for quantitative measurement of the dopant concentration profile in production semiconductor devices. We calibrate the sMIM using a doped calibration sample prior to performing the measurements on an "unknown" production device. We utilize nanoscale C-V curves to establish a calibration curve for both n- and p-type carriers in a single reference and apply the calibration curve to an "unknown" device presenting the measurements in units of doping concentration. The calibrated results are compared to SRP measurements on the same area of the device.

1. Introduction

Scanning probe microscopy (SPM) based electrical measurement techniques [1], such as scanning capacitance microscopy (SCM) [2], scanning spreading resistance (SSRM) [3] and scanning microwave microscopy (SMM) [4] have shown value for the profiling of dopants in semiconductor samples, but suffer from significant limitations. Conventional SCM is performed using a resonant circuit originally invented by RCA in the 1980s [3]. SSRM is restricted to samples that provide a DC path from the probe tip to ground. Scanning microwave impedance microscopy (sMIM) is an emerging technique that has the potential to displace conventional SCM, and other electrical SPM techniques, for the profiling of dopants in semiconductor samples with deep sub-micron spatial resolution [5]. Application of microwave frequencies to image doped semiconductors has a long history, but only more recently been successfully integrated with AFM for imaging.

1.1. Experimental arrangement

Fig. 1 shows a schematic diagram of sMIM hardware. The sMIM measurements discussed here were performed using commercially available atomic force microscopes (AFM) configured to capture the output signals from the sMIM hardware [6]. The *sMIM* electronics couples a 3 GHz microwave signal to the AFM probe tip *via* a 50-Ω impedance interface module and a micro-fabricated coaxial transmission line in a custom-designed, shielded, metal SPM probe. The reflected microwave signal is amplified and demodulated by the sMIM electronics providing two analog signals representing the Real and Imaginary components of the complex reflection coefficient into the SPM controller where it is synchronized with the topography during scanning [7]. With the addition of a lock-in amplifier, the sMIM can provide the dC/dV amplitude and phase signals correlating with the doping concentration and carrier type, respectively, of a doped semiconductor analogous to SCM.

In an sMIM experiment, microwaves are coupled through a custom AFM cantilever to the probe [8] where they interact as evanescent waves with the portion of the sample immediately under the tip. A fraction of the microwaves is reflected and the amplitude and phase (or equivalently, the real and imaginary parts) of the reflection are determined by the local electrical properties of the sample. For a linear sample the permittivity and conductivity determine the reflection, while for non-linear sample like a doped semiconductor, the tip-bias-dependent-depletion-layer structure contributes significantly. SMM is a related technique that also uses microwave interactions to probe electrical properties. Recent work has shown promising preliminary results despite using unshielded probes [9].

The sMIM-C data improves with a dual pass scan when used for quantification applications. The sample is scanned using contact-mode where the first pass follows the surface topography and a second pass is made 100's of nanometers above the sample surface following the same topography forming a constant offset height image. The difference of these two images is used for subsequent analysis for quantification. The difference image reduces effects from stray capacitance and drift. As a result, sMIM measurements can provide valuable nano-scale

* Corresponding author.
E-mail address: amster@primenanoinc.com (O. Amster).

http://dx.doi.org/10.1016/j.microrel.2017.07.082
0026-2714/

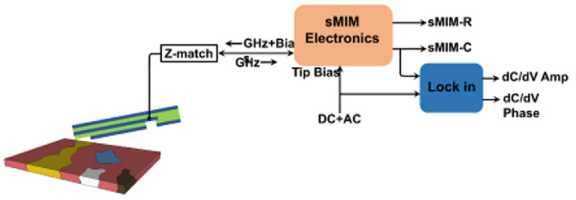

Fig. 1. Schematic of the sMIM electronics, matching circuit with shielded coaxial line to the probe-sample interface.

information about semiconductor devices, processes and defects. Results of dopant-level characterization are presented here.

2. Discussion of results

2.1. sMIM-C quantification validation

Quantitative profiling of the dopants in a semiconductor sample with sMIM requires calibration of the sMIM-C signal. The most practical method uses a "known" dopant calibration sample, such as those available from IMEC [10] and Infineon [11]. Fig. 2 shows sMIM-C, C-V response for an Infineon dopant calibration sample where the fast-axis is x-position and the slow-axis is DC bias. The vertical black dashed lines mark the center of the doped regions in x. A black set of asterisks mark the scan at which a 0 V bias occurs. Fig. 2b. shows the profile of sMIM-C acquired at that bias. This profile has peaks in sMIM-C at the x-locations of the doped regions.

These peaks of sMIM-C give the "log-linear" calibration data for sMIM-C in terms of log doping, as shown in Fig. 3. The numerical calibration derived from linear fits shown in Fig. 3 are:

$$\mathrm{sMIM_P} = 0.176 * \log_{10}(\mathrm{N_A}) - 2.48, \mathrm{CC} = 0.993 \quad (1)$$

$$\mathrm{sMIM_N} = 0.183 * \log_{10}(\mathrm{N_D}) - 2.55, \mathrm{CC} = 0.999 \quad (2)$$

The fits neglect the points for the highest doping concentrations, of both N- and P-types, because they are next to each other at in the center of the collection of doped stripes, and corrupt the measurements of each

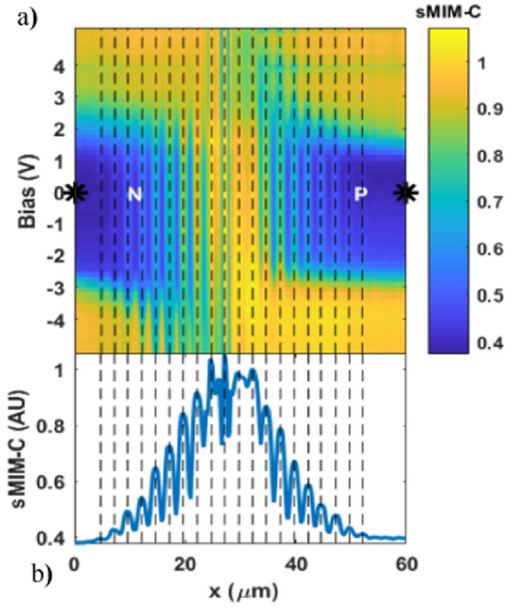

Fig. 2. Data collected as an image, a) has the fast-scan axis as x and the "slow-scan axis" as DC tip bias. Black asterisks mark the scan line that is at a bias of 0 V in panel a, And panel b shows the profile of sMIM-C acquired at that bias. These peaks of sMIM-C give the "log-linear" calibration data for sMIM-C in terms of log doping, as shown in the figure below.

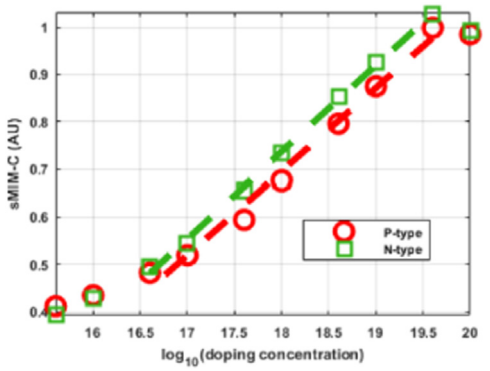

Fig. 3. The numerical calibration derived from linear fits to the doped regions for both n-type and p-type. The specific points are taken from the sMIM-C values at 0 V bias as shown in Fig. 2b, having been extracted from values in Fig. 2a along the line between the asterisks.

other. The points for the two lowest doping levels are likely corrupted by noise. In retrospect, longer integration times would have been appropriate.

Fig. 3 clearly shows a monotonic behavior for both p-type and n-type dopants on same axis. The higher doping concentrations are to the right of the chart, giving a higher sMIM-C signal, and the less doped material gives a lower signal.

Fig. 4 shows sMIM-C, C-V curves extracted along the vertical lines in Fig. 2; a) for the p-type regions and b) for the n-type regions. These data are proportional to C-V, with accumulation on the left and inversion on the right for the p-type and accumulation on the right and inversion on the left for the n-type regions. The values in accumulation were forced to be the same *a posteriori*, for ease of comparison to the reader.

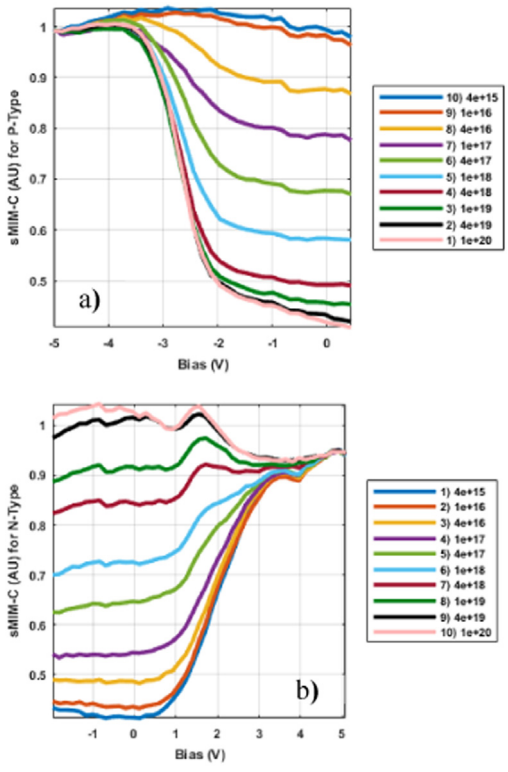

Fig. 4. sMIM-C extracted along vertical lines in Fig. 2 for a) p-type and b) n-type doped regions as a function of bias. These data are proportional to C(V), with accumulation on the left and inversion on the right for the p-type and *vice-versa* for the n-type. The values in accumulation were forced to be the same *a posteriori*.

Please cite this article as: O. Amster, et al., Practical quantitative scanning microwave impedance microscopy, Microelectronics Reliability (2017), http://dx.doi.org/10.1016/j.microrel.2017.07.082